

# Asphericity analysis using corneal wavefront and topographic meridional fits

## Samuel Arba-Mosquera

University of Valladolid  
Instituto de Oftalmobiología Aplicada  
Refractive Surgery and Quality of Vision  
Valladolid, E-47004 Spain  
and  
SCHWIND eye-tech-solutions  
Research and Development  
Mainparkstrasse 6-10  
Kleinostheim, D-63801 Germany

## Jesús Merayo-Llodes

University of Valladolid  
Instituto de Oftalmobiología Aplicada  
Refractive Surgery and Quality of Vision  
Valladolid, E-47004 Spain

## Diego de Ortueta

Augenzentrum Recklinghausen  
Recklinghausen, Germany

**Abstract.** The calculation of corneal asphericity as a 3-D fit renders more accurate results when it is based on the corneal wavefront aberrations rather than on the corneal topography of the principal meridians. A more accurate prediction could be obtained for hyperopic treatments compared to myopic treatments. We evaluate a method to calculate corneal asphericity and asphericity changes after refractive surgery. Sixty eyes of 15 consecutive myopic patients and 15 consecutive hyperopic patients ( $n=30$  each) are retrospectively evaluated. Preoperative and 3-month-postoperative topographic and corneal wavefront analyses are performed using corneal topography. Ablations are performed using a laser with an aberration-free profile. Topographic changes in asphericity and corneal aberrations are evaluated for a 6-mm corneal diameter. The induction of corneal spherical aberrations and asphericity changes correlates with the achieved defocus correction. Preoperatively as well as postoperatively, asphericity calculated from the topography meridians correlates with asphericity calculated from the corneal wavefront in myopic and hyperopic treatments. A stronger correlation between postoperative asphericity and the ideally expected/predicted asphericity is obtained based on aberration-free assumptions calculated from corneal wavefront values rather than from the meridians. In hyperopic treatments, a better correlation can be obtained compared to the correlation in myopic treatments. Corneal asphericity calculated from corneal wavefront aberrations represents a 3-D fit of the corneal surface; asphericity calculated from the main topographic meridians represents a 2-D fit of the principal corneal meridians. Postoperative corneal asphericity can be calculated from corneal wavefront aberrations with higher fidelity than from corneal topography of the principal meridians. Hyperopic treatments show a greater accuracy than myopic treatments. © 2010 Society of Photo-Optical Instrumentation Engineers. [DOI: 10.1117/1.3382910]

Keywords: asphericity; wavefront; topography; aberration; Zernike.

Paper 09474RRR received Oct. 19, 2009; revised manuscript received Feb. 11, 2010; accepted for publication Feb. 22, 2010; published online Apr. 12, 2010.

## 1 Introduction

A strong tendency toward the use of asphericity parameters in refractive surgery can be observed<sup>1,2</sup> in reporting measurements<sup>3,4</sup> and mean values,<sup>5-7</sup> and using different descriptors (asphericity quotient  $Q$ , conic constant  $K$ , eccentricity  $e$ ,  $p$  value  $p$ , or shape factor  $E$ ) or measuring the effects of refractive treatments on corneal asphericity.<sup>8,9</sup>

Topographically guided treatments,<sup>10</sup> wavefront-driven treatments,<sup>11</sup> wavefront-optimized treatments,<sup>12</sup> asphericity-preserving treatments,<sup>13</sup> and  $Q$ -factor profiles<sup>14</sup> have been proposed as solutions to provide patients with the best possible functional vision. All these approaches behave differ-

ently and exert different effects on the postoperative asphericity.

An analysis of corneal topography involves fitting the measured data to geometric models, usually by inclusion of a simple regular surface and a polynomial adjustment of the extra components not covered by the simple regular surface basis.

In this paper, two simple methods to calculate corneal asphericity—based on the corneal wavefront and on the asphericity of the two principal meridians—are compared and the question of whether the corneal wavefront alone is a useful metric to evaluate the corneal asphericity in refractive surgery is addressed. For the purpose of this study, the methods presented were applied to a patient population treated with laser *in situ* keratomileusis (LASIK).

Address all correspondence to: Samuel Arba-Mosquera, SCHWIND eye-tech-solutions, Research and Development, Mainparkstrasse 6-10, Kleinostheim, D-63801 Germany. Tel: 496027508274; Fax: 496027508208; E-mail: sarbamo@cofis.es

## 2 Materials and Methods

Retrospective analysis of 60 eyes, including 15 consecutive patients each with myopia and hyperopia, treated at Augenzentrum Recklinghausen (Recklinghausen, Germany) was performed. Preoperative and 3-month-postoperative data are reported.

All operations were performed by one surgeon (DdO). LASIK flaps were created with a Carriazo-Pendular microkeratome<sup>15</sup> (SCHWIND eye-tech-solutions GmbH, Kleinostheim, Germany). An ESIRIS system<sup>16</sup> (SCHWIND eye-tech-solutions GmbH) set for an optical zone of 6.25 mm was used to perform the ablations with aberration-free profiles<sup>17</sup> without nomogram adjustments. This profile does not deliver wavefront-guided ablation targeting zero aberrations after surgery. Rather, the ablation profile itself is aberration free, which means that no aberration is induced by the ablation, so that the preexisting aberrations are preserved.

Preoperative findings as well as outcomes at 3 months postoperatively included manifest refraction, topography, corneal aberrometry, and complications.

Using Keratron-Scout<sup>18</sup> (Optikon2000, Rome, Italy) topographical analysis of the radii of curvature and asphericities of the principal meridians and the corneal wavefront aberrations to the seventh Zernike order was performed preoperatively and 3 months postoperatively.

Classical relationships between different asphericity descriptors<sup>19</sup> were calculated using the formulas

$$p \equiv Q + 1 \equiv 1 - E = 1 - e^2,$$

$$Q \equiv p - 1 \equiv -E = -e^2,$$

$$E \equiv 1 - p \equiv -Q = e^2,$$

$$e = \sqrt{1 - p} \equiv \sqrt{-Q} \equiv \sqrt{SF},$$

where

$$p < 0 \Rightarrow \text{hyperbola},$$

$$p = 0 \Rightarrow \text{parabola},$$

$$0 < p < 1 \Rightarrow \text{prolate ellipse},$$

$$p = 1 \Rightarrow \text{sphere},$$

$$p > 1 \Rightarrow \text{oblate ellipse}.$$

However, asphericity is a dependent parameter with “non-linear” behavior, i.e., it has no meaning, if the apical curvature is not taken into consideration. Any asphericity descriptor can be used, however, to obtain consistent results and interpretations, but the computing cannot be reduced to linear arithmetic. The asphericity descriptor used throughout the study was the  $p$  value ( $p$ ).

Topographic asphericity was computed using two methods. The first was the topographic method based on the principal

meridians.<sup>20</sup> Considering the mean corneal asphericity of a series of corneal asphericities, the mean asphericity<sup>20</sup> was computed as

$$\bar{p} = \frac{\sum_{i=1}^m (p_i/R_i^3)}{[\sum_{i=1}^m (1/R_i)]^3} m^2, \quad (1)$$

where  $\bar{p}$  is the mean asphericity,  $p_i$  are the asphericity factors,  $R_i$  are the apical radii of curvature, and  $m$  is the sample size.

To average the asphericity of the two main meridians under consideration of their curvature, Eq. (1) reduces to

$$p = 4 \frac{p_s/R_s^3 + p_f/R_f^3}{(1/R_s + 1/R_f)^3}, \quad (2)$$

where  $p$  is the corneal  $p$  value;  $p_s$  and  $p_f$  are the  $p$  values of the steep and flat principal meridians, respectively; and  $R_s$  and  $R_f$  are the apical radii of curvature of the steep and flat principal meridians.

This method represents a calculation of mean asphericity derived from  $m$  meridional radii and asphericities obtained from 2-D fits of the corneal meridians.

The second method investigated was the corneal wavefront method:<sup>20</sup>

$$p = \frac{768R^3(C_4^0\sqrt{5} - 5C_6^0\sqrt{7} + 45C_8^0)}{OZ^4(1-n)}, \quad (3)$$

where  $p$  is the corneal  $p$  value;  $C[4,0]$ ,  $C[6,0]$ , and  $C[8,0]$  are the radially symmetric terms of the corneal Zernike expansion;  $R$  is the apical radius of the corneal curvature;  $n$  is the corneal refractive index; and  $OZ$  is the analyzed diameter of the corneal Zernike expansion.

This method represents a calculation of the mean asphericity derived from corneal wavefront data obtained from a 3-D fit of the corneal surface. The radially symmetric terms of the corneal Zernike expansion,  $C[4,0]$ ,  $C[6,0]$ , and  $C[8,0]$ , were calculated from the radially symmetric terms of the corneal Zernike expansion<sup>21</sup> of the surface elevation of a Cartesian oval ( $C_{co}[4,0]$ ,  $C_{co}[6,0]$ , and  $C_{co}[8,0]$ ) plus the radially symmetric terms of the corneal wavefront aberration, as provided by the videokeratoscope ( $C_{cw}[4,0]$  and  $C_{cw}[6,0]$ ).

Also, the ideally expected topographic asphericity assumed from aberration-neutral conditions was calculated using two methods. First, the ideally expected principal meridians of the topographic method,

$$p_{\text{exp}} = p_{\text{co}} + \frac{p_{\text{pre}} - p_{\text{co}}}{[1 + (RSEq_{cp}/n - 1)]^3}, \quad (4)$$

where  $p_{\text{exp}}$  is the predicted corneal  $p$  value;  $p_{\text{co}}$  and  $p_{\text{pre}}$  are the  $p$  values of a Cartesian oval and the preoperative cornea, respectively;  $R$  is the apical radius of curvature of the preoperative cornea; and  $SEq_{cp}$  is the spherical equivalent to be corrected at the corneal plane.

In this paper, the term “ideally expected” is understood to mean “predicted values” if the aberration-free condition were strictly fulfilled.

The second method employed was the ideally expected corneal wavefront method, again using Eq. (3), with  $R$  as the postoperative predicted apical radius of curvature.

**Table 1** Preoperative and postoperative data.

	Myopic Group	Hyperopic Group	All Treatments
No. of treated eyes (patients)	30 (15)	30 (15)	60 (30)
Preoperative SEq±StdDev (D)	-3.18±1.21	+2.48±1.41	-0.32±3.15
Preoperative cylinder±StdDev (D)	0.50±0.48	0.65±0.79	0.58±0.66
Postoperative SEq±StdDev (D)	+0.19±0.28	+0.04±0.35	+0.11±0.32
Postoperative cylinder±StdDev (D)	0.05±0.08	0.11±0.15	0.08±0.13
Predictability <0.50 D (%)	90%	100%	95%
Predictability <1.00 D (%)	100%	100%	100%

Note that the ideally expected corneal wavefront method using Eq. (3) can easily be further applied to any target condition, simply by setting the radially symmetric terms of the corneal wavefront aberration ( $C_{cw}[4,0]$  and  $C_{cw}[6,0]$ ) to the desired value.

Optical errors, represented by wavefront aberrations, as described by Zernike polynomials<sup>22</sup> and coefficients in the Optical Society of America (OSA) standard<sup>23</sup> were analyzed for 6-mm diameters.

### 2.1 Clinical Evaluation

Each cornea underwent four consecutive measurements preoperatively as well as at the 3-month follow-up examination, summing up to a total of 240 measurements. For every cornea, the four corresponding topographies were analyzed using both methods, and the corresponding mean value according to Eqs. (1) or (3) was used as representative asphericity of that cornea with each method.

### 2.2 Repeatability of Methods

Following preoperative calculation of the  $p$  values with both methods, a global analysis of the behavior of the term  $pR^{-3}$  was performed. According to Eqs. (1) and (3), it constitutes a term to be operated on in a simple linear manner. The four corresponding values of each cornea were averaged for both methods, and a global standard deviation value was calculated across the 240 measurements for each method using the formula

$$\text{StdDev}_{\text{Global}} = \left\{ \frac{\sum_{a=1}^A \sum_{b=1}^B [p_{a,b} R_{a,b}^{-3} - (\sum_{c=1}^B p_{a,c} R_{a,c}^{-3}) / B]^2}{AB - 1} \right\}^{1/2}, \quad (5)$$

where  $a$  runs over the number of corneas of the sample ( $A=60$ ), and  $b$  and  $c$  run over the number of corresponding measurements for each cornea ( $B=4$ ).

### 2.3 Statistical Analysis

We used  $t$  tests for statistical analysis, with  $P < 0.05$  considered as significant.

## 3 Results

### 3.1 Refractive Outcomes

In both myopic and hyperopic eyes, spherical equivalent (SEq) and cylinder were reduced to subclinical values at 3 months postoperatively (range  $-0.50$  to  $+0.75$  D for defocus and  $0.00$  to  $0.75$  D for astigmatism), and 95% of eyes ( $n=57$ ) were within  $\pm 0.50$  D of the attempted correction (Table 1 and Fig. 1).

### 3.2 Corneal Spherical Aberrations

In the myopic group, the preoperative primary corneal spherical aberration ( $C[4,0]$ ) was  $+0.243 \pm 0.098 \mu\text{m}$  (mean  $\pm$  standard deviation), and changed to  $+0.319 \pm 0.132 \mu\text{m}$  at 3 months postoperatively ( $P < 0.01$ ). In the hyperopic group,  $C[4,0]$  was  $+0.201 \pm 0.118 \mu\text{m}$  and changed to  $-0.006 \pm 0.139 \mu\text{m}$  at 3 months postoperatively ( $P < 0.001$ ) (Table 2).

Induced corneal spherical aberration, defined as the difference in postoperative corneal spherical aberration minus the preoperative value, was significant for primary and secondary spherical aberrations ( $P < 0.001$  for both) and significantly correlated with the achieved defocus correction for primary and secondary spherical aberrations ( $r^2=0.65$ ,  $P < 0.001$  for primary spherical aberration and  $r^2=0.59$ ,  $P < 0.001$  for secondary spherical aberration). The rate of induced corneal spherical aberration per defocus (regression slope) was  $-0.045 \mu\text{m}/\text{D}$  for primary spherical aberration and  $-0.001 \mu\text{m}/\text{D}$  for secondary spherical aberration at 6 mm (Fig. 2).

### 3.3 Corneal Asphericity

In the myopic group, the mean preoperative corneal asphericity calculated from the principal meridians was  $+0.79$ , whereas the mean corneal asphericity calculated from the corneal wavefront was  $+0.89$ . In the hyperopic group, the mean preoperative corneal asphericity calculated from the principal meridians was  $+0.81$ , whereas the mean corneal asphericity calculated from the corneal wavefront was  $+0.82$  (Table 3).

The preoperative corneal asphericity calculated from the corneal wavefront significantly correlated with the corneal asphericity calculated from the principal meridians in both the

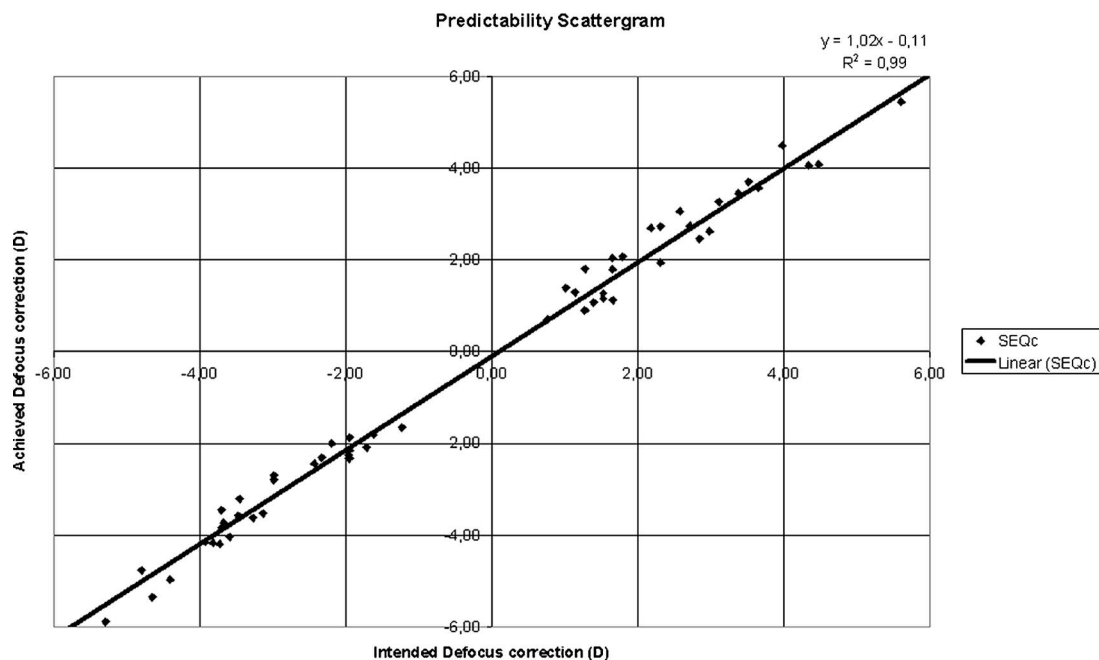


Fig. 1 Predictability scattergram.

myopic and the hyperopic group ( $r^2=0.84$ ,  $P<0.001$  for the myopic group;  $r^2=0.87$ ,  $P<0.001$  for the hyperopic group). Further, the regression slope was 1.01 for the myopic group and 1.09 for the hyperopic group (Fig. 3).

In the myopic group, the mean postoperative corneal asphericity calculated from the principal meridians was +1.24, whereas the mean corneal asphericity calculated from the corneal wavefront was +1.13. In the hyperopic group, the mean postoperative corneal asphericity calculated from the principal meridians was +0.39, whereas the mean corneal asphericity calculated from the corneal wavefront was +0.47 (Table 3).

Postoperatively, the corneal asphericity calculated from the corneal wavefront values significantly correlated with the corneal asphericity calculated from the principal meridians in both the myopic and the hyperopic group ( $r^2=0.81$ ,  $P<0.001$  for the myopic group;  $r^2=0.85$ ,  $P<0.001$  for the hyperopic group). Further, the regression slope was 0.51 for the myopic group and 0.88 for the hyperopic group (Fig. 4).

### 3.4 Corneal Asphericity Changes

For myopia, the ideally expected postoperative  $p$  value calculated from the principal meridians was +0.87, compared to +0.98 in the wavefront-based calculation (Table 3). The postoperative asphericity did not correlate with the predicted asphericity when calculated from the meridians ( $r^2=0.07$ ,  $P=0.2$ ), and showed a weak but significant correlation with the ideally expected asphericity when calculated from the wavefront ( $r^2=0.12$ ,  $P=.05$ ). Further, the regression slope was +0.68 in a corneal wavefront-based calculation.

For hyperopia, the predicted postoperative asphericity calculated from the principal meridians was +0.76, compared to +0.75 in a wavefront-based calculation (Table 3). The postoperative asphericity was significantly correlated with the ideally expected asphericity when calculated from the meridians ( $r^2=0.39$ ,  $P<0.001$ ), and strongly correlated with the predicted asphericity when calculated from the wavefront

Table 2 Corneal wavefront aberration data reported for 6-mm analysis diameter.

	Myopic Group	Hyperopic Group	All Treatments
Preoperative primary SphAb±StdDev ( $\mu\text{m}$ )	+0.243±0.098	+0.201±0.118	+0.221±0.111
Preoperative secondary SphAb±StdDev ( $\mu\text{m}$ )	0.000±0.003	0.000±0.002	0.000±0.002
Postoperative primary SphAb±StdDev ( $\mu\text{m}$ )	+0.319±0.132	-0.006±0.139	+0.154±0.214
Postoperative secondary SphAb±StdDev ( $\mu\text{m}$ )	+0.003±0.003	-0.004±0.004	-0.0001±0.005
Induced primary SphAb per diopter ( $\mu\text{m}$ )	-0.031	-0.048	-0.043
Induced secondary SphAb per diopter ( $\mu\text{m}$ )	-0.001	-0.001	-0.001

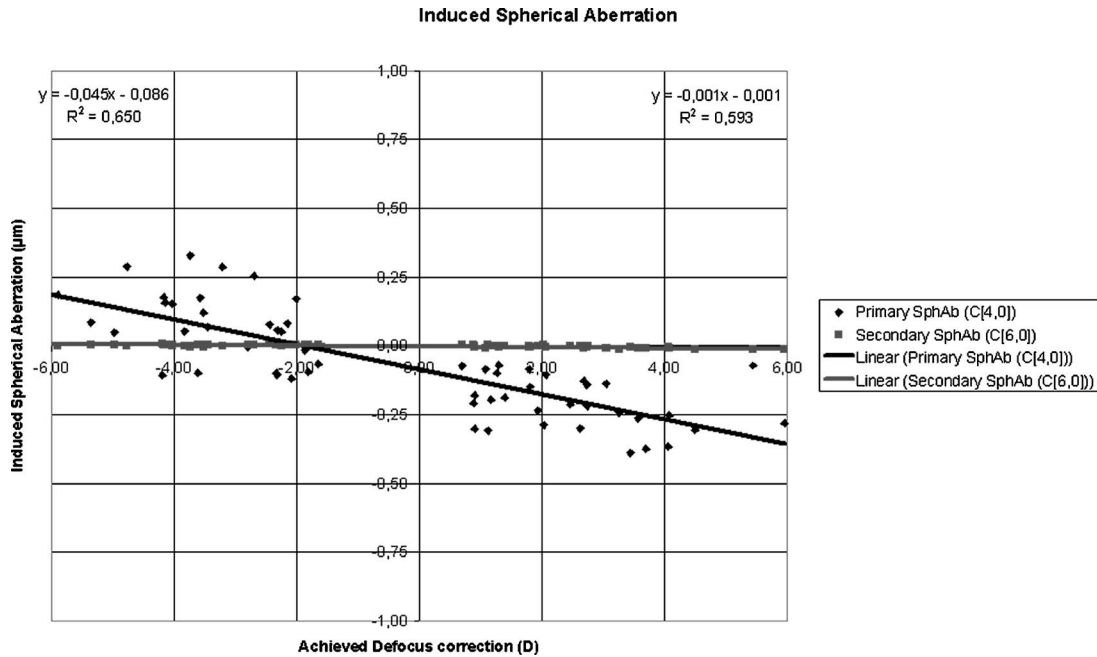


Fig. 2 Induced spherical aberration.

( $r^2=0.51$ ,  $P<0.001$ ). Further, the regression slope was +0.67 when calculated from the principal meridians and +0.71 when calculated from the corneal wavefront.

Combining the results of both groups, the ideally expected postoperative asphericity calculated from the principal meridians was +0.81 and that calculated from the corneal wavefront +0.85 (Table 3). The postoperative asphericity was significantly but weakly correlated with the predicted asphericity when calculated from the principal meridians ( $r^2=0.17$ ,  $P<0.05$ ), and showed a strong correlation with the ideally expected corneal asphericity when calculated from the corneal wavefront ( $r^2=0.37$ ,  $P<0.001$ ). Further, the regression slope was +1.44 in a principal-meridian-based calculation and +1.19 in a corneal-wavefront-based calculation (Fig. 5).

### 3.5 Repeatability of the Corneal Asphericity

The global standard deviation was  $0.0003 \text{ mm}^{-3}$  for the meridional method, compared to  $0.0001 \text{ mm}^{-3}$  for the corneal wavefront method ( $P<0.05$ ).

## 4 Discussion

We used the  $p$  value as the asphericity descriptor throughout this study. The reason for this choice was not a preference for the  $p$  value over other asphericity descriptors. In fact, using the identities and equalities described, similar equations could have been derived for any asphericity descriptor. Our aim was the consistent use of one descriptor and to use the classical relationships between descriptors combined with Eqs. (1) and (3), or (4) to derive descriptor-specific equations for computing the mean values, asphericity out of the corneal wavefront, or estimation of the postoperative asphericity, respectively. Note that using simple arithmetic, the average of a parabola ( $p=0$ ) with an apical curvature of 7 mm and a sphere ( $p=1$ ) with a radius of curvature of 8 mm would be  $p=0.5$  (i.e.,  $e=0.71$ ). For the same surfaces, however, an averaged parabola ( $e=1$ ) and an averaged sphere ( $e=0$ ) would be  $e=0.5$  (i.e.,  $p=0.75$ ) and not 0.71. Using our model, the result would always be  $p=0.41$  or  $e=0.77$ .

Table 3 Asphericity data.

	Myopic Group	Hyperopic Group	All Treatments
Preoperative $p$ value from meridians	+0.79	+0.81	+0.80
Preoperative $p$ value from corneal wavefront	+0.89	+0.82	+0.85
Postoperative $p$ value from meridians	+1.24	+0.39	+0.73
Postoperative $p$ value from corneal wavefront	+1.13	+0.47	+0.74
Expected/predicted $p$ value from meridians	+0.87	+0.76	+0.81
Expected/predicted $p$ value from corneal wavefront	+0.98	+0.75	+0.85

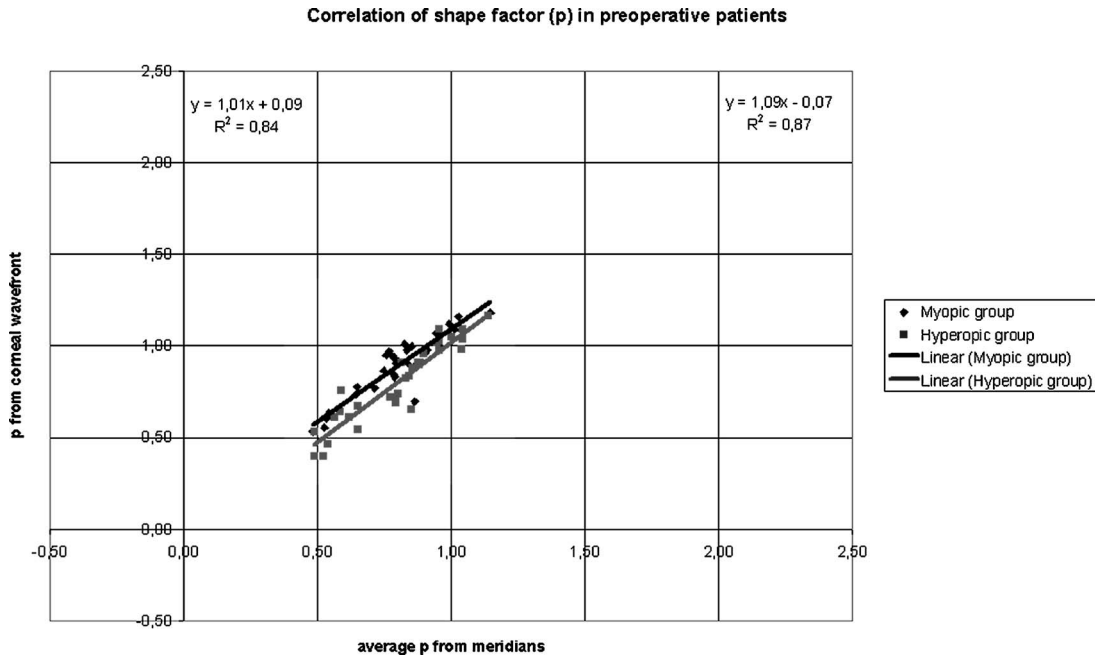


Fig. 3 Preoperative asphericity.

In particular, the corneal wavefront method benefits from avoidance of complicated nonlinear effects in the analysis. Once the Zernike expansion of the corneal wavefront aberration is known, the corresponding coefficients can be linearly averaged, added, or subtracted, or any other linear operation can be performed, and finally the asphericity value can be computed in the desired descriptor.

By analyzing topographic changes, a highly significant correlation between the asphericity calculated from corneal

wavefront and from the principal meridians could be observed in both the myopic and the hyperopic group preoperatively as well as postoperatively (Figs. 3 and 4).

To assess the agreement between the methods, a Bland-Altman plot was created<sup>24</sup> (Fig. 6) that showed that the asphericity calculation with the two methods does not produce equivalent results. Corneal-wavefront-based calculation showed an asphericity with an average of 0.05 units higher compared to the calculation based on the principal meridians.

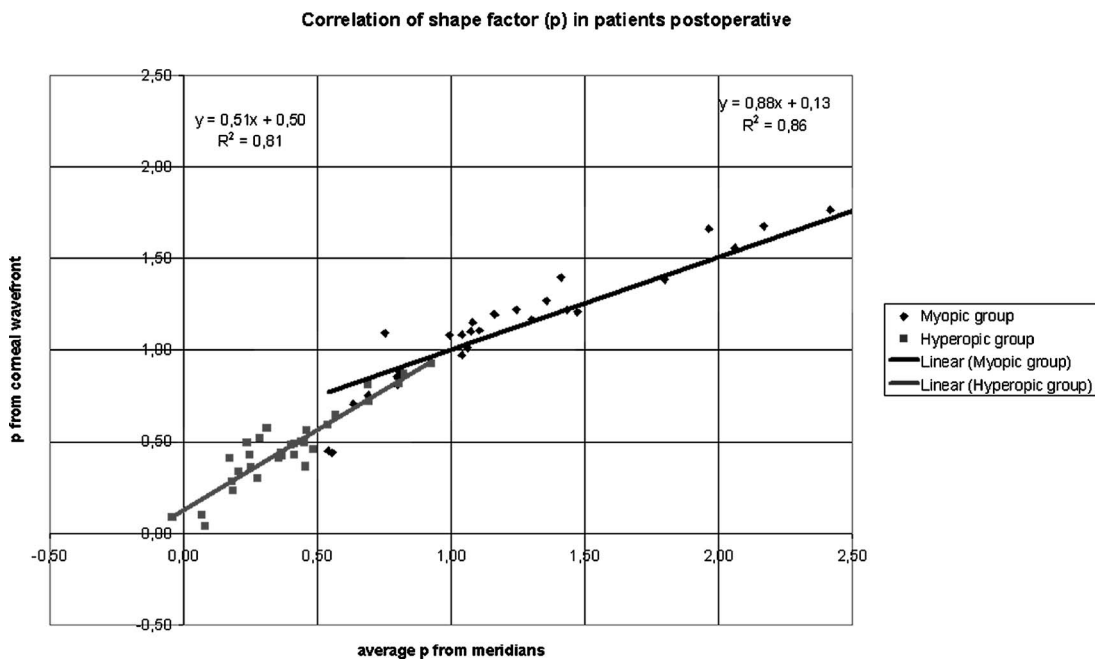


Fig. 4 Postoperative asphericity.

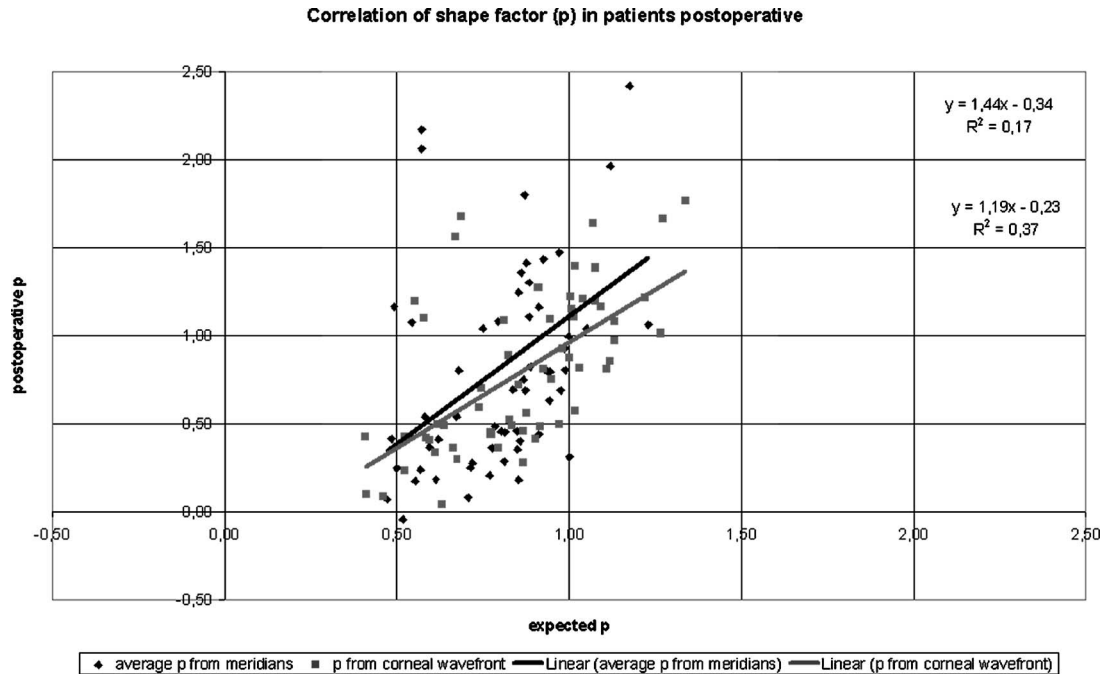


Fig. 5 Ideally expected postoperative asphericity.

Moreover, the difference between the two methods correlated weakly but significantly with the measured value ( $r^2=0.11$ ;  $P < 0.05$ ).

The wavefront method proved to be superior to the meridional method, since the aberration coefficients were computed from much denser data sampling (all corneal points within a disk with a 6-mm diameter), and not only from two meridians. However, the conclusion that if many meridians were

included in the “meridional” method, the results would approach those of the “wavefront” method is misleading.

Another weakness of the “two-meridians method” is that both meridians are usually selected based on their respective curvature, i.e., the main origin of astigmatism. These two meridians closely represent the highest and lowest meridional curvatures of a cornea, but their corresponding asphericities

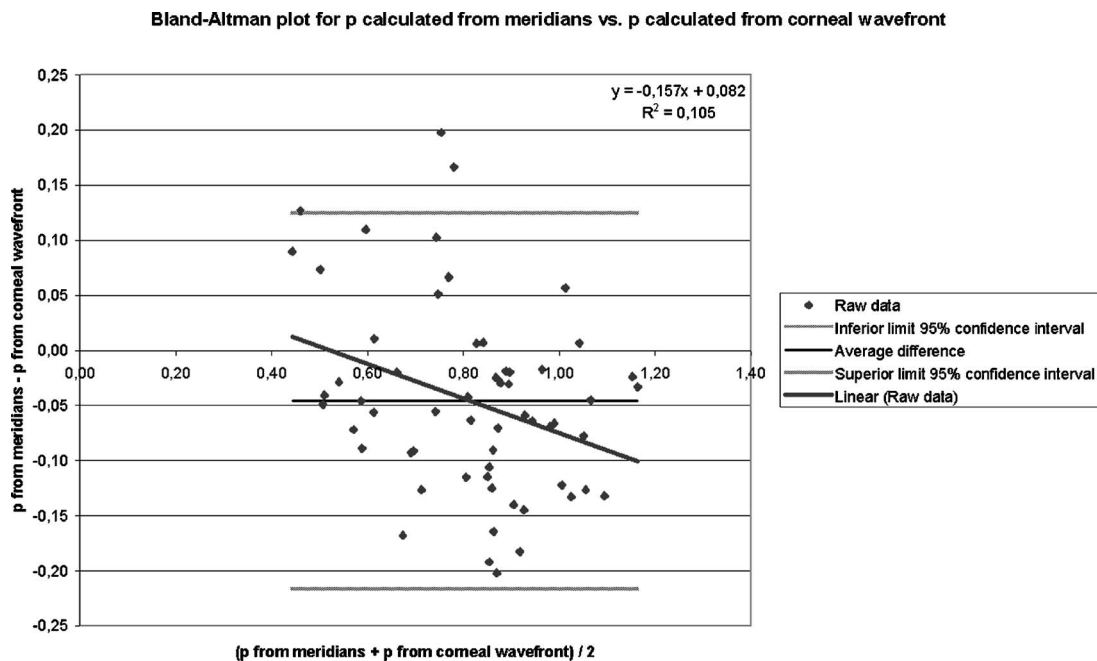


Fig. 6 Bland-Altman plot for  $p$  value calculated from the meridians versus  $p$  value calculated from the corneal wavefront.

do not necessarily represent the highest and lowest meridional asphericities of that cornea.

In the groups in this study, the postoperative asphericity deviated more from the preoperative asphericity than predicted by aberration-neutral assumptions calculated from the principal meridians as well as the corneal wavefront. Also, the postoperative asphericity showed a stronger correlation with the asphericity predicted from aberration-neutral assumptions when calculated from corneal wavefront than from the meridians (Fig. 5).

The preoperative mean corneal asphericity in myopic eyes calculated with the two methods showed a similar result, which, however, was not as consistent as the result found in the hyperopic group. The fact that both the amount of corneal astigmatism, which was larger in the hyperopic group (Table 1), and the offset between the corneal vertex and the pupil center, which was also larger in the hyperopic group,<sup>25</sup> may play a role here.

Note also that the Zernike decomposition predicted only 37% of the variance of asphericity change, i.e., there is high scatter (Fig. 5) and there is a tendency toward higher asphericity, which is also reflected by the induction of spherical aberrations.

A possible cause of measured differences in induced asphericity between calculated and real postoperative corneas could be the fact that changes in radius and changes in asphericity were analyzed separately. This is strictly valid only if both parameters are independent, however, there is a very strong correlation between changes in asphericity and changes in radius. This correlation may have two origins: (1) artifacts of the measurement or the fitting procedure or (2) a real correlation in changes of radius and asphericity in the cornea, possibly due to biomechanical constraints. Similarly to Pérez-Escudero et al.<sup>26</sup> and to the findings of a paper presented earlier by the authors,<sup>27</sup> a topography describing a perfect rotationally symmetric ellipsoid with radius  $R=7.87$  mm and asphericity  $p=0.75$ , which are typical values for the anterior corneal surface, was created. Subsequently, random noise was added to the elevation. Normally distributed random noise with a standard deviation of  $3\ \mu\text{m}$  was employed, which is the same order of magnitude observed in measurements with the Scout videokeratoscope. This results in a data set similar to the experimental data sets, however, without the particularities that may be specific to our setup. One hundred such surfaces were created using the same base ellipsoid and changing only the noise. Subsequently, this surface was fitted. The results show that the parameters of the base ellipsoid are well recovered by the mean, but that there is a strong correlation between changes in  $R$  and changes in  $p$ . The same applies to correlations between changes in  $1/R$  and changes in  $p/R^3$ . These correlations are not particular to our specific fitting procedure, rather are they a general characteristic of fits to surfaces that derive from ellipses. These correlations are an artifact caused by the fit's sensitivity to measurement noise and are probably common to all fits of ellipse-based surfaces. Both the biomechanical response of the stroma and wound healing could also contribute to this phenomenon.

Navarro et al.<sup>28</sup> proposed a relatively simple general model to represent the corneal surface in its canonical form with respect to the axes of corneal symmetry. One limitation of the

Navarro et al. model is that it assumes that the orientations of the principal curvatures, i.e., the steepest and flattest radii, related to corneal toricity, correspond to the orientations of the principal asphericities. Kiely et al.<sup>3</sup> investigated this problem in 1982, using a model more general than an ellipsoid, which was oriented according to the instrument axes.

The mean asphericity is a convenient parameter for the comparison of different eyes and characterization of spherical aberration of a conicoid, but it cannot be a substitute for corneal topography. There are circumstances when knowledge of the asphericity in the two principle meridians might be more useful for vision correction than the mean asphericity. However, as already mentioned, the asphericity of the two principle meridians might not be the minimum and maximum meridional asphericities for that cornea. In this respect, Navarro's corneal model presents a good basis for corneal topography, representing a realistic anatomic situation and employing additional terms of Zernike expansion to describe extra surface deformation of real corneas. Zernike terms would resolve the issue, with the strongest asphericity not being along the principal meridians. On the other hand, the quadratic surface basis for the corneal surface will provide only an aberration-free basis with the instrument on axis and will not be as realistic as the Navarro et al. ellipsoid. As a consequence, the quadratic surface will require larger additional Zernike terms to represent the real corneal topography.

Corneal description should not be limited to the mean asphericity, related to spherical aberration, when corneal topography in Zernike terms gives much more general information on corneal aberrations. However, if a simple corneal model based on asphericity is of interest for reasons of simplicity, we advocate for calculating the mean asphericity from the corneal wavefront rather than from the asphericity of the two principle meridians. This simplification is less complicated but essentially similar to a reduction of the wavefront aberration map to a generic description based on  $n$  weight coefficients of the Zernike expansion. This approach is no attempt to discredit the full details of corneal topography or the optical description provided by Zernike polynomials. Rather the aim is to reduce the complexity of the description to an appropriate minimal set of parameters.<sup>29,30</sup>

In particular cases, spherical aberration could be described by way of comparison of the Zernike terms with radial symmetry, such as  $C[4,0]$  and  $C[6,0]$ ; to be more accurate, the contribution from the power terms with pure  $\rho^4$  and  $\rho^6$  in the corneal topography expansion ( $\rho$  is the normalized pupil radius). In this way, a higher order aspheric surface could be characterized rather than limiting analysis to the mean asphericity that corresponds to a conicoid surface, which in some cases is a poor approximation for high-order aspheric corneas.

Another possible model, which is also direct and simple and combines the advantages of other different models is that of a quadric surface free on the space, i.e., oriented according to the natural corneal axes, however, with a fixed constant asphericity corresponding to the Cartesian oval for the refractive index ( $p$  value of +0.472 with a corneal refractive index of 1.376), without astigmatism, to determine the apical curvature and the corneal axis. The modeled surface would always be a surface free of on-axis aberrations for any particular apical curvature. The residual component would be adjusted to a

Zernike polynomial expansion, because it would directly represent the surface aberration of the corneal wavefront.

This paper suggests that the corneal wavefront alone is a useful metric to evaluate the optical quality of an ablation in refractive surgery, and a useful metric to evaluate corneal asphericity. The corneal wavefront can be used effectively to analyze laser refractive surgery, avoiding complicated nonlinear effects in the analysis. On these grounds, this method has the potential to replace or perhaps supplement currently used methods of asphericity analysis based on simple averaging of asphericity values.

### Acknowledgments

The authors thank Alfonso Pérez Escudero for fruitful discussions and his time and expertise to critically review this manuscript. Samuel Arba-Mosquera is an employee of SCHWIND eye-tech-solutions. Diego de Ortueta is a consultant for SCHWIND eye-tech-solutions.

### References

- D. Gatinel, M. Haouat, and T. Hoang-Xuan, "A review of mathematical descriptors of corneal asphericity," *J. Fr. Ophthalmol.* **25**, 81–90 (2002).
- A. Calossi, "Corneal asphericity and spherical aberration," *J. Refract. Surg.* **23**, 505–514 (2007).
- P. M. Kiely, G. Smith, and L. G. Carney, "The mean shape of the human cornea," *Opt. Acta* **29**, 1027–1040 (1982).
- M. Sheridan and W. A. Douthwaite, "Corneal asphericity and refractive error," *Ophthalmic Physiol. Opt.* **9**, 235–238 (1989).
- A. Stojanovic, L. Wang, M. R. Jankov, T. A. Nitter, and Q. Wang, "Wavefront optimized versus custom-Q treatments in surface ablation for myopic astigmatism with the WaveLight ALLEGRETTO laser," *J. Refract. Surg.* **24**, 779–789 (2008).
- J. R. Jimenez, R. G. Anera, J. A. Díaz, and F. Pérez-Ocón, "Corneal asphericity after refractive surgery when the Munnerlyn formula is applied," *J. Opt. Soc. Am. A Opt. Image Sci. Vis.* **21**, 98–103 (2004).
- P. Vinciguerra and F. I. Camesasca, "Treatment of hyperopia: a new ablation profile to reduce corneal eccentricity," *J. Refract. Surg.* **18**, S315–317 (2002).
- D. Gatinel, T. Hoang-Xuan, and D. T. Azar, "Determination of corneal asphericity after myopia surgery with the excimer laser: a mathematical model," *Invest. Ophthalmol. Visual Sci.* **42**, 1736–1742 (2001).
- R. G. Anera, J. R. Jiménez, L. Jiménez del Barco, J. Bermúdez, and E. Hita, "Changes in corneal asphericity after LASER in situ keratomileusis," *J. Cataract Refractive Surg.* **29**, 762–768 (2003).
- J. L. Alio, J. I. Belda, A. A. Osman, and A. M. Shalaby, "Topography-guided laser in situ keratomileusis (TOPOLINK) to correct irregular astigmatism after previous refractive surgery," *J. Refract. Surg.* **19**, 516–527 (2003).
- M. Mrochen, M. Kaemmerer, and T. Seiler, "Clinical results of wavefront-guided laser in situ keratomileusis 3 months after surgery," *J. Cataract Refractive Surg.* **27**, 201–207 (2001).
- M. Mrochen, C. Donetzky, C. Wüllner, and J. Löffler, "Wavefront-optimized ablation profiles: theoretical background," *J. Cataract Refractive Surg.* **30**, 775–785 (2004).
- D. Z. Reinstein, D. R. Neal, H. Vogelsang, E. Schroeder, Z. Z. Nagy, M. Bergt, J. Copland, and D. Topa, "Optimized and wavefront guided corneal refractive surgery using the Carl Zeiss Meditec platform: the WASCA aberrometer, CRS-Master, and MEL80 excimer laser," *Ophthalmol. Clin. North. Am.* **17**, 191–210 (2004).
- T. Koller, H. P. Iseli, F. Hafezi, M. Mrochen, and T. Seiler, "Q-factor customized ablation profile for the correction of myopic astigmatism," *J. Cataract Refractive Surg.* **32**, 584–589 (2006).
- D. de Ortueta, "Planar flaps with the Carriazo-Pendular microkeratome," *J. Refract. Surg.* **24**, 322 (2008).
- M. C. Arbelaez, C. Vidal, B. A. Jabri, and S. Arba Mosquera, "LASIK for myopia with aspheric 'aberration neutral' ablations using the ESIRIS laser system," *J. Refract. Surg.* **25**, 991–999 (2009).
- D. de Ortueta, S. Arba Mosquera, and H. Baatz, "Comparison of standard and aberration-neutral profiles for myopic LASIK with the SCHWIND ESIRIS platform," *J. Refract. Surg.* **25**, 339–349 (2009).
- R. Mattioli and N. K. Tripoli, "Corneal geometry reconstruction with the Keratron videokeratographer," *Optom. Vision Sci.* **74**, 881–894 (1997).
- ISO "Ophthalmic instruments—corneal topographers," ISO Standard 19980:2005.
- D. De Ortueta and S. Arba-Mosquera, "Mathematical properties of asphericity: a method to calculate with asphericities," *J. Refract. Surg.* **24**, 119–121 (2008).
- D. Gatinel, J. Malet, T. Hoang-Xuan, and D. T. Azar, "Corneal asphericity change after excimer laser hyperopic surgery: theoretical effects on corneal profiles and corresponding Zernike expansions," *Invest. Ophthalmol. Visual Sci.* **45**, 1349–1359 (2004).
- F. Zernike, "Diffraction theory of the knife-edge test and its improved form, the phase-contrast method," *Mon. Not. R. Astron. Soc.* **94**, 377–384 (1934).
- L. N. Thibos, R. A. Applegate, J. T. Schwiegerling, R. Webb, and VSIA Standards Taskforce Members, "Standards for reporting the optical aberrations of eyes," *J. Refract. Surg.* **18**, S652–S660 (2002).
- D. G. Altman and J. M. Bland, "Measurement in medicine: the analysis of method comparison studies," *Statistician* **32**, 307–317 (1983).
- M. C. Arbelaez, C. Vidal, and S. Arba-Mosquera, "Clinical outcomes of corneal vertex versus central pupil references with aberration-free ablation strategies and LASIK," *Invest. Ophthalmol. Visual Sci.* **49**, 5287–5294 (2008).
- A. Pérez-Escudero, C. Dorronsoro, and S. Marcos, "An artifact in fits to conic-based surfaces," E-pub only: arXiv:0905.0814v1 (2009).
- S. Arba-Mosquera and D. de Ortueta, "Analysis of optimized profiles for 'aberration-free' refractive surgery," *Ophthalmic Physiol. Opt.* **29**, 535–548 (2009).
- R. Navarro, L. González, and J. L. Hernández, "Optics of the average normal cornea from general and canonical representations of its surface topography," *J. Opt. Soc. Am. A* **23**, 219–232 (2006).
- P. R. Preussner and J. Wahl, "Simplified mathematics for customized refractive surgery," *J. Cataract Refractive Surg.* **29**, 462–470 (2003).
- P. R. Preussner, J. Wahl, and C. Kramann, "Corneal model," *J. Cataract Refractive Surg.* **29**, 471–477 (2003).